Quantum Irregular Spectrum in a Corresponding Classically Chaotic Lattice Spin System

K. Nakamura and Y. Nakahara
Fukuoka Institute of Technology, Higashi-ku, Fukuoka 811-02, Japan

and

A. R. Bishop
Theoretical Division and Center for Nonlinear Studies, Los Alamos National Laboratory, Los Alamos, New Mexico 87545
(Received 26 November 1984)

The quantum spectrum is studied in a corresponding classically nonintegrable triangular three-spin system with antiferromagnetic exchange coupling. A critical energy E_c is identified numerically. Irregularly distributed (bandlike) levels and well-separated clusters of (localized) levels appear below and above E_c, respectively. The statistical average of second-order differences of eigenvalues shows a scaling behavior when the spin magnitude is increased towards $+\infty$.

PACS numbers: 05.45.+b, 05.50.+q, 75.10.Jm

Despite accumulating studies on completely integrable lattice spin systems,[1-3] information on nonintegrable ones is much less complete. For instance, although a quantum spin $S=\frac{1}{2}$ one-dimensional XYZ model is completely integrable, the integrability of its generalized $S>\frac{1}{2}$ versions remains an open question: The classical ($S=+\infty$) limit is a nonintegrable dynamical system, as will be confirmed below. Thus, there arises a question about the nature of intermediate semiclassical regions bridging the $S=\frac{1}{2}$ integrable quantum limit and the $S=+\infty$ nonintegrable classical limit. In this Letter, we investigate the quantum irregular spectrum for a three-spin chain with periodic boundary conditions (i.e., a triangular lattice spin system), and with anisotropic (XXZ) antiferromagnetic exchange coupling. Although the number of spins is small, we will exploit the advantage of being able to handle a large range of spin magnitude S. This kind of small spin cluster can actually be relevant in real materials such as trinucleus complexes or short-range-ordered three-spin clusters of Fe^{2+} ions around each Rb^+ ion in a triangular $RbFeCl_3$ antiferromagnet.

First, we present brief results for the classical limit, showing Poincaré surfaces of section for regular and/or irregular orbits. Second, quantum energy levels in the semiclassical regions for $S\leq 36\frac{1}{2}$ are reported and analyzed. Finally, we point out an apparent scaling law satisfied by the statistical average of second-order differences of eigenvalues for increasing (large) S.

The Hamiltonian we consider is

$$H=\sum_{\langle i,j\rangle} J(\mathbf{S}_i\cdot\mathbf{S}_j+\sigma S_i^z S_j^z),\quad 1\leq i,j\leq 3, \tag{1}$$

where $J(>0)$ and $\sigma(-1\leq\sigma\leq 0)$ are the antiferromagnetic exchange constant and the anisotropy parameter, respectively. In the following, we take $J=1$ without loss of generality. The Hamiltonian in Eq. (1) holds for both classical and quantum spins. In the classical limit, $\mathbf{S}_j$ is a three-component vector obeying the equation of motion

$$d\mathbf{S}_j/dt=\{\mathbf{S}_j,H\}=\mathbf{S}_j\times(-\delta H/\delta\mathbf{S}_j), \tag{2}$$

where $\{A,B\}$ is a Poisson bracket. Since the magnitude of each spin is conserved, Eq. (2) describes the dynamics in six-dimensional phase space. For $\sigma=0$, three components of $\mathbf{T}=\sum_{j=1}^{3}\mathbf{S}_j$ (more rigorously, appropriate combinations of them) are constants of motion, while for $\sigma\neq 0$, $T^z=\sum_{j=1}^{3}S_j^z$ alone is conserved. When we note the first integral of motion, i.e., energy E, the effective dimensionality of the phase space becomes $2(=6-3-1)$ and $4(=6-1-1)$ for $\sigma=0$ and for $\sigma\neq 0$, respectively. Therefore the former case is integrable and the latter one may be nonintegrable. We choose $\mathbf{S}_j^2=1$ and $T^z=0$ throughout the following classical treatment.

The classical ground state of the system in Eq. (1) with $\sigma<0$ is characterized by the 120° structure in a basal (S^x-S^y) plane. So we take as initial data for Eq. (2) those determined by polar and azimuthal angles of each spin: $\theta_1^{(0)}=\pi/2$, $\phi_1^{(0)}=\alpha$; $\theta_2^{(0)}=\pi/2+\beta$, $\phi_2^{(0)}=2\pi/3$; $\theta_3^{(0)}=\pi/2-\beta$, $\phi_3^{(0)}=4\pi/3$; where α and β are arbitrary parameters denoting basal disorder and off-plane angles, respectively. The energy E is then

$$E=-\cos\alpha\cos\beta-(\sigma+1)+(\sigma+\tfrac{1}{2})\cos^2\beta.$$

E is decreased from high-energy regions towards the ground-state energy $E_g^{cl}=-1.5$ with $\alpha=\beta=0$. For each fixed value E, several sets of angle variables (α,β) are taken. The resulting dynamics is analyzed by use of Poincaré surfaces of section specified by $dS_1^z/dt=0$. Projections onto the (S_1^x-S_1^y) plane are given in Figs. 1(a)–1(c) for $\sigma=-0.3$. (Note that the sections are still three-dimensional for $\sigma\neq 0$.) From these figures we find that most of the orbits are regular Kolmogorov-Arnol'd-Moser (KAM) tori[4-6] in higher-energy regions and that irregular orbits dominate KAM orbits in lower-energy regions. We have checked the irregularity of orbits via the study of power spectra. Irregular orbits are found to persist in

the vicinity of $E = E_g^{cl}$. These results are the reverse of those for conventional classical Hamiltonian dynamics.[4,5] Our results are qualitatively similar throughout the range $-1 \leq \sigma < 0$; only periodic orbits can exist for the integrable case $\sigma = 0$.

We now proceed to the quantum treatment of the system (1). We have examined a distribution of quantum energy levels.[6] (All questions of time dependence are omitted.) Diagonalization of the matrix constructed from Eq. (1) is facilitated by use of the C_{3v} symmetry of the system and the planar symmetry in spin space. Basic "kets" are classified by a set of quantum numbers: wave number K $(0, 2\pi/3, 4\pi/3)$, parity $(+1, -1)$, and magnetization T^z (integer, half integer). An example of basic kets with a definite set of quantum numbers ($T^z = M + M' + M''$) is

$$\tfrac{1}{2}[\tfrac{1}{3}\sqrt{3}\{|S,M\rangle_1 \otimes |S,M'\rangle_2 \otimes |S,M''\rangle_3 + e^{iK}|S,M''\rangle_1 \otimes |S,M\rangle_2 \otimes |S,M'\rangle_3 + e^{2iK}|S,M'\rangle_1 \otimes |S,M''\rangle_2 \otimes |S,M\rangle_3\} \pm \tfrac{1}{3}\sqrt{3}\{M \leftrightarrow M'\}], \quad (3)$$

when M, M', and M'' take different values. We calculate matrix elements for general spin by noting that $\langle S,M'|S_j^z|S,M\rangle_j = M\delta_{M',M}$ and

$$\langle S,M'|S_j^{\pm}|S,M\rangle_j = [(S \mp M)(S \pm M + 1)]^{1/2}\delta_{M',M\pm1}.$$

A huge matrix is thus decomposed into small block matrices. In the following, we concentrate on the manifold $K = 0$, parity $= +1$, and $T^z = \frac{1}{2}$. Energies are divided by $S(S+1)$ so that these scaled energies become densely populated in a finite energy range for $S \gg 1$.

In Figs. 2(a)–2(c), 276 energy levels for $S = 22\frac{1}{2}$ are presented with $\sigma = -0.3$, -0.1, and 0.0, respectively. 153 energy levels for $S = 16\frac{1}{2}$ with $\sigma = -0.3$ are also shown in Fig. 2(a). In Figs. 2(a) and 2(b), a critical energy E_c is evident (see arrows). For $E < E_c$, levels are irregularly distributed and bandlike, while for $E > E_c$ they consist of stairs of well-separated clustered (localized) levels. E_c, showing little dependence on S for $S \gg 1$ [compare two-level diagrams in Fig. 2(a)], decreases as the nonintegrability parameter σ approachs 0. In Fig. 2(c), E_c coincides with the energy of the quantum ground state and only regular stairs of clustered degenerate levels are observed, where degenerate levels can be classified by a new quantum number [eigenvalue of $\mathbf{T}^2 = (\sum_{j=1}^{3}\mathbf{S}_j)^2$]. The coexistence of bandlike regions and clustered (localized) regions for $\sigma < 0$ is reminiscent of Anderson localization.[7] Although the present system, Eq. (1), includes no extrinsic randomness, the intrinsic chaos

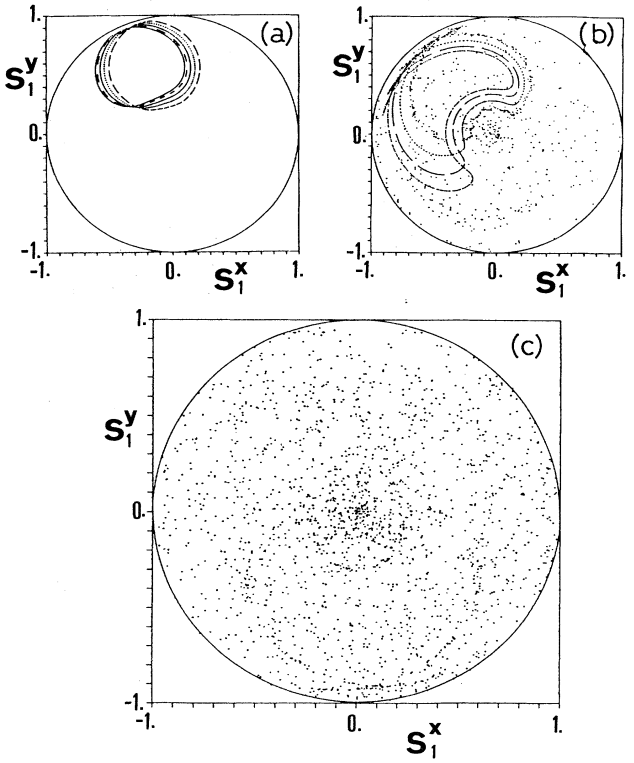

FIG. 1. Projection onto the $(S_1^x$-$S_1^y)$ plane of the Poincaré surface of section for $\sigma = -0.3$. Five orbits with initial angles $\beta = n\pi/50$ $(n = 1, 2, 3, 4, 5)$ are shown: (a) $E = -1.175$. (b) $E = -1.206$. Only a single orbit with $\beta = \pi/10$ is shown. (c) $E = -1.210$.

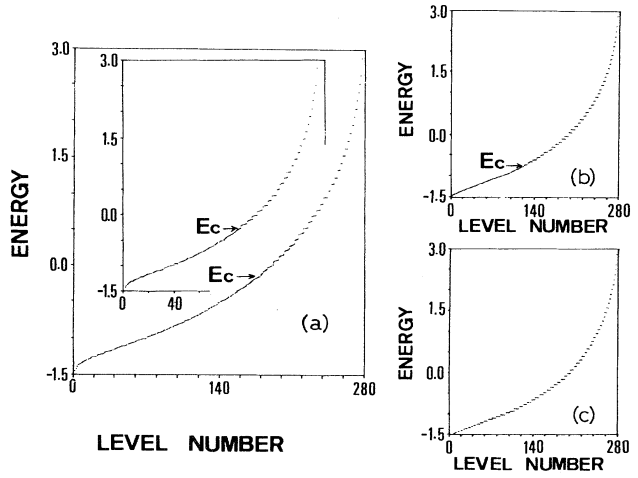

FIG. 2. Energy levels for $S = 22\frac{1}{2}$ with $K = 0$, parity $= +1$ and $T^z = \frac{1}{2}$. (a) $\sigma = -0.3$; (b) $\sigma = -0.1$; (c) $\sigma = 0.0$. Energy levels for $S = 16\frac{1}{2}$ are also shown in the inset of (a). Energies are scaled by $S(S+1)$.

(nonintegrability) may play a similar role: Irregular level distributions and stairs of clustered levels in Fig. 2(a) are quantum manifestations of the classical chaos in Figs. 1(b) and 1(c) and of KAM orbits in Figs. 1(a) and 1(b), respectively. Direct one-to-one correspondences between quantum irregular spectrum and classical chaos, however, cannot easily be established,[8] although regular stairs of clustered levels in Fig. 2(c) are obviously quantum counterparts of periodic orbits in the integrable ($\sigma=0$) classical case.

To evaluate the sensitivity of eigenvalues to the nonintegrability parameter σ, we calculate the second-order differences $\Delta^2E/\Delta\sigma^2$ (i.e., the local curvatures of the σ-dependent quantum energy diagram) defined by

$$\frac{\Delta^2E}{\Delta\sigma^2}\equiv\frac{[E(\sigma+\Delta\sigma)-2E(\sigma)+E(\sigma-\Delta\sigma)]}{(\Delta\sigma)^2}. \quad (4)$$

This was originally proposed by Pomphrey,[9] but statistical averages of Eq. (4) are examined in our study. In the case of $\sigma=-0.3$ with $\Delta\sigma=5\times10^{-4}$, we present the S dependence of $\langle|\Delta^2E/\Delta\sigma^2|\rangle$, i.e., the mean value of $|\Delta^2E/\Delta\sigma^2|$, and that of the standard deviation

$$\langle(\Delta^2E/\Delta\sigma^2-\langle\Delta^2E/\Delta\sigma^2\rangle)^2\rangle^{1/2}$$

in Figs. 3(a) and 3(b), respectively. Here, angular brackets imply the average over levels within individual energy ranges in Figs. 3(a) and 3(b). For $E<-0.75$, both the mean value and standard deviation basically grow with increasing S. For $-0.75\leqslant E<-0.25$, on the contrary, the possibility of their growth with S can hardly be expected despite the presence of spikes in histograms. For $E\geqslant-0.25$, increasing S keeps the mean value almost constant and decreases the standard deviation. In our classical treatment for $\sigma=-0.3$, widespread chaos can be observed only for $E\lesssim-0.75$ and particularly for $-1.25\lesssim E\lesssim-1.0$, as suggested in Figs. 1(b) and 1(c). Therefore, $E_c'(\sim-0.75)$, below which the statistical averages of $\Delta^2E/\Delta\sigma^2$ grow with increasing S, might be a more promising critical energy than E_c [~-0.25; see Fig. 2(a)] in characterization of the quantum version of classical chaos.

Finally we define a dimensionless standard deviation

$$g(S)\equiv\frac{\langle(\Delta^2E/\Delta\sigma^2-\langle\Delta^2E/\Delta\sigma^2\rangle)^2\rangle^{1/2}}{|\langle\Delta^2E/\Delta\sigma^2\rangle|}. \quad (5)$$

In the common range $-1.25\leqslant E<-1.0$ where the average is taken, the S dependence of $g(S)$ is shown in Fig. 4 for $\sigma=-1.0$, -0.3, -0.1, and 0.0. In the range $-0.25\leqslant E<0.0$, the similar dependence for $\sigma=-0.3$ is also given. The former and latter ranges lie below E_c' [more precisely, $E_c'(\sigma)$] except for $\sigma=0.0$ and well above E_c', respectively. Figure 4 indicates the existence of a scaling law of the form

$$g(\Lambda S)/g(S)=\Lambda^{\beta(\sigma)}, \quad (6)$$

where Λ is an arbitrary multiplicative factor. $\beta(\sigma)=4.69$ in the range $-1.25\leqslant E<-1.0$ for $\sigma=-0.3$ and increases when σ approaches 0 so long as the energy range lies below $E_c'(\sigma)$. $\beta>0$ suggests a fractal nature of the σ-dependent quantum energy diagram for $S\gg1$, which corresponds to classical chaos. On the other hand, $\beta(\sigma)=-0.13$ and -0.71

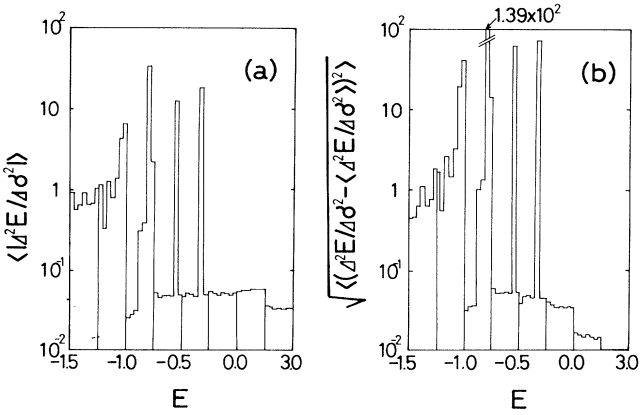

FIG. 3. (a) S dependence of $\langle|\Delta^2E/\Delta\sigma^2|\rangle$. (b) S dependence of $\langle[(\Delta^2E/\Delta\sigma^2)-\langle\Delta^2E/\Delta\sigma^2\rangle]^2\rangle^{1/2}$. Lower-energy side ($-1.5\leqslant E\leqslant0.0$) is divided into six energy ranges, while the higher side ($0.0\leqslant E\leqslant3.0$) is divided into two ranges. In the histogram in each energy region, $S=8\frac{1}{2},12\frac{1}{2},\ldots,32\frac{1}{2}$ from the left at intervals of 4. Energies are scaled by $S(S+1)$.

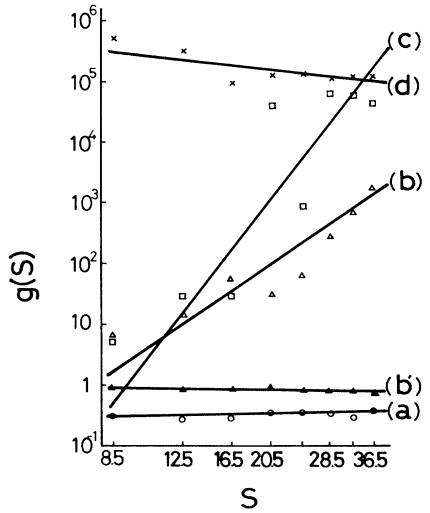

FIG. 4. S dependence of $g(S)$ in logarithmic scales. Average over $-1.25\leqslant E<-1.0$: line a, $\sigma=-1.0$ (circles); line b, $\sigma=-0.3$ (open triangles); line c, $\sigma=-0.1$ (squares); line d, $\sigma=0.0$ (crosses). Average over $-0.25\leqslant E\leqslant0.0$: line b', $\sigma=-0.3$ (filled triangles). Energies are scaled by $S(S+1)$.

in the ranges $-0.25 \leq E < 0.0$ for $\sigma = -0.3$ and $-1.25 \leq E < -1.0$ for $\sigma = 0.0$, respectively. $\beta \leq 0$ implies a smooth σ-dependent energy diagram for $S >> 1$, which corresponds commonly to classical KAM tori and periodic orbits.

In conclusion, the semiclassical quantum irregular spectrum of a corresponding chaotic lattice spin system demonstrates a situation reminiscent of Anderson localization. The dimensionless statistical average of second-order differences of eigenvalues exhibits in large-spin regions a scaling behavior, with the exponent strongly dependent on the nonintegrability parameter σ.

The authors wish to thank H. Mori and K. Kawasaki for valuable discussions.

[1]L. A. Takhtadzhan and L. D. Faddeev, Usp. Mat. Nauk. **34**, No. 5, 13 (1979) [Russ. Math. Surv. **34**, 11 (1979)]; H. B. Thacker, Rev. Mod. Phys. **53**, 253 (1981).

[2]For recent status, see papers in "Dynamical Problems in Soliton Systems," Proceedings of the Seventh Kyoto Summer Institute, Kyoto, 1984, edited by S. Takeno (to be published); K. Nakamura, T. Sasada, and A. R. Bishop, J. Phys. C **16**, 3771 (1983).

[3]Recent studies have even questioned the validity of "universal" scaling forms in nonintegrable systems, e.g., B. McCoy, to be published.

[4]M. Hénon and C. Heiles, Astron. J. **69**, 73 (1964).

[5]M. Tabor, in *Advances in Chemical Physics, Vol. 48,* edited by I. Prigogine and S. A. Rice (Wiley, New York, 1981); A. J. Lichtenberg and M. A. Lieberman, *Regular and Stochastic Motion* (Springer, Berlin, 1983).

[6]M. V. Berry and M. Tabor, Proc. Roy. Soc. London, Ser. A **356**, 375 (1977); S. W. McDonald and A. N. Kaufman, Phys. Rev. Lett. **42**, 1189 (1979); G. M. Zaslavsky, Phys. Rep. **80**, 157 (1981); P. Pechukas, Phys. Rev. Lett. **51**, 943 (1983).

[7]See, E. Abrahams, P. W. Anderson, D. C. Licciardello, and T. V. Ramakrishnan, Phys. Rev. Lett. **42**, 673 (1979).

[8]D. Farrelly, Phys. Lett. **104A**, 63 (1984); M. V. Berry, Phys. Lett. **104A**, 306 (1984).

[9]N. Pomphrey, J. Phys. B **7**, 1909 (1974); R. A. Pullen and A. R. Edmonds, J. Phys. A **14**, L477 (1981).